Vacancy ordering in Co_3AlC_x alloys: A first-principles study

C. Jiang*
Structure/Property Relations Group (MST-8), Los Alamos National Laboratory, Los Alamos, New Mexico 87545, USA
(Received 2 July 2008; revised manuscript received 4 August 2008; published 22 August 2008)

Ordering of structural vacancies in nonstoichiometric Co_3AlC_x alloys has been studied using a combination of first-principles total-energy calculations, a cluster expansion technique, and Monte Carlo simulations. In the proximity of the experimentally observed composition of $x \sim 0.59$, our exhaustive ground-state search yields two stable vacancy-ordered structures: a cubic $Co_3AlC_{0.5}$ phase and a trigonal $Co_3AlC_{0.667}$ phase. By performing finite-temperature Monte Carlo simulations, the order-disorder transition temperatures of $Co_3AlC_{0.5}$ and $Co_3AlC_{0.667}$ are predicted to be ~1925 and ~1630 K, respectively.

DOI: 10.1103/PhysRevB.78.064206 PACS number(s): 61.66.Dk

I. INTRODUCTION

It is well known that commercial Ni-based superalloys are strengthened by $L1_2$-Ni_3Al compound that forms coherent cuboidal precipitates within the fcc Ni-based solid solution. In contrast, development of Co-base superalloys is much more difficult due to the absence of a stable $L1_2$-Co_3Al phase in the Co-Al binary system.[1] Nevertheless, experimental investigations suggest that there do exist a stable Co_3AlC_x compound with cubic perovskite ($E2_1$)-based structure in the Co-Al-C ternary system.[2–5] Since the $E2_1$ structure is crystallographically very similar to that of the $L1_2$ structure, the Co_3AlC_x compound is considered a potential strengthener for a new class of Co-based superalloys.

In the ideal $E2_1$ Co_3AlC unit cell (see Fig. 1), the three Co atoms occupy the face centers (3*c* site), the Al atom occupies the cube corner (1*a* site), and the C atom occupies the cube center (1*b* site). Experimentally, it has been established that not all the 1*b* sites are occupied by C atoms and thus the nonstoichiometric compound is denoted as Co_3AlC_x with x measured to be ~0.59.[2] Instead of randomly occupying the carbon sublattice, those structural vacancies can undergo long-range ordering to form superstructures. For transition-metal carbides such as Co_3AlC_x, knowledge of such ordering phenomenon is indispensable since it can sensitively control their many important physical and mechanical properties.[6–8]

In this paper, we apply a generalized lattice model to predict the low-temperature vacancy-ordered structures in Co_3AlC_x alloys. A cluster expansion (CE) (Refs. 9–13) characterizing the distribution of C atoms and vacancies on the 1*b* sites is constructed from first-principles calculated total energies of a series of Co_3AlC_x ($x=0-1$) ordered structures. Using our cluster expansion, an exhaustive ground-state search is performed to find the lowest-energy configurations at $T=0$ K. Subjecting our cluster expansion to canonical Monte Carlo simulations, the order-disorder transition temperatures of those ground-state-ordered structures are also obtained and compared with experiments.

II. METHODOLOGY

A. First-principles method

First-principles total-energy calculations are performed using the all-electron Blöchl's projector augmented wave (PAW) approach,[14] as implemented in VASP.[15] The exchange-correlation functional is described within the Perdew–Burke–Ernzerhof generalized gradient approximation (PBE-GGA).[16] The *k*-point meshes for Brillouin-zone sampling are constructed using the Monkhorst–Pack scheme[17] and the total number of *k* points times the total number of atoms per unit cell is at least 5000 for all structures. The cutoff energy for plane-wave basis set is set at 500 eV. Spin-polarized calculations are performed to account for the ferromagnetic nature of Co. By computing the quantum-mechanical forces and stress tensor, the unit-cell volume and shape as well as all internal atomic positions of all structures are fully relaxed using a conjugate-gradient scheme.

The formation energy (per f.u.) of a Co_3AlC_x alloy relative to the composition-weighted average of the end members is defined as

$$\Delta H = E(Co_3AlC_x) - (1-x)E(Co_3Al) - xE(Co_3AlC), \quad (1)$$

where $E(Co_3Al)$, $E(Co_3AlC)$, and $E(Co_3AlC_x)$ are the first-principles calculated total energies of the constituent $L1_2$ Co_3Al, $E2_1$ Co_3AlC, and the corresponding alloy, each relaxed to their equilibrium geometries, respectively.

B. Cluster expansion technique

For a binary $A_{1-x}B_x$ substitutional alloy, many properties such as energy are dependent on the *configuration*, i.e., the substitutional arrangement of the *A* and *B* atoms on an un-

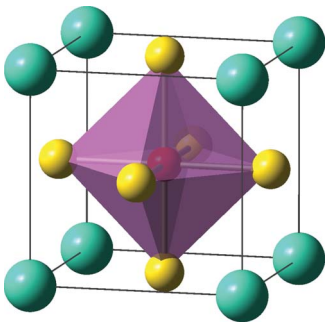

FIG. 1. (Color online) The ideal cubic perovskite ($E2_1$) Co_3AlC structure. Cyan, yellow, and red spheres represent Al, Co, and C atoms, respectively.

TABLE I. ECIs of the present cluster expansion together with the definitions of all the figures considered. Vertices of figures are given in units of a, the $E2_1$ lattice parameter.

Cluster type	Figure designation	D_f	J_f (meV)	$D_f J_f$ (meV)	Vertices			
Empty	J_0	1	−121.21	−121.21				
Point	J_1	1	67.75	67.75	(0.5, 0.5, 0.5)			
Pair	J_2	3	40.06	120.17	(0.5, 0.5, 0.5)	(−0.5,0.5,0.5)		
	K_2	6	−12.23	−73.38	(0.5, 0.5, 0.5)	(0.5,−0.5,−0.5)		
	L_2	4	−3.07	−12.28	(0.5, 0.5, 0.5)	(−0.5,−0.5,−0.5)		
	M_2	3	10.06	30.19	(0.5, 0.5, 0.5)	(0.5, 2.5, 0.5)		
	N_2	12	−0.17	−1.98	(0.5, 0.5, 0.5)	(−0.5,2.5,0.5)		
Triplet	J_3	12	−2.06	−24.66	(0.5, 0.5, 0.5)	(0.5,−0.5,0.5)	(0.5,−0.5,−0.5)	
	K_3	8	0.17	1.33	(0.5, 0.5, 0.5)	(−0.5,0.5,−0.5)	(0.5,−0.5,−0.5)	
	L_3	24	−0.20	−4.70	(0.5, 0.5, 0.5)	(0.5,−0.5,0.5)	(−0.5,−0.5,−0.5)	
	M_3	3	−9.93	−29.78	(0.5, 0.5, 0.5)	(0.5, 1.5, 0.5)	(0.5, 2.5, 0.5)	
	N_3	12	−0.76	−9.06	(0.5, 0.5, 0.5)	(0.5,1.5,−0.5)	(0.5, 2.5, 0.5)	
Quadruplet	J_4	3	−1.15	−3.45	(0.5, 0.5, 0.5)	(0.5,0.5,−0.5)	(0.5,−0.5,0.5)	(0.5,−0.5,−0.5)
	K_4	8	1.21	9.67	(0.5, 0.5, 0.5)	(0.5,0.5,−0.5)	(−0.5,0.5,−0.5)	(0.5,−0.5,−0.5)
	L_4	2	1.32	2.65	(0.5, 0.5, 0.5)	(−0.5,−0.5,0.5)	(−0.5,0.5,−0.5)	(0.5,−0.5,−0.5)
	M_4	24	0.18	4.34	(0.5, 0.5, 0.5)	(−0.5,0.5,0.5)	(0.5,−0.5,0.5)	(−0.5,−0.5,−0.5)
	N_4	24	1.90	45.62	(0.5, 0.5, 0.5)	(0.5,−0.5,0.5)	(0.5,−0.5,−0.5)	(−0.5,−0.5,−0.5)

derlying parent lattice (in our case, the $1b$ sites). For a system with N atoms, there can be 2^N possible number of configurations, which is an astronomically large number when N is large. In order to search for $T=0$ K ground-state structures or to compute finite-temperature thermodynamic properties, it is necessary to explore such a huge configurational space, which is clearly computationally prohibitive using direct first-principles methods. To overcome such difficulties, we adopt the CE technique[9–13] in the present study. Within this method, one characterizes a configuration σ on an underlying parent lattice by assigning pseudospin variables to each site: $S_i=-1(+1)$ if an A (B) atom sits at site i (in our case, $S_i=-1$ for C atoms and +1 for vacancies). The formation energy of *any* lattice configuration $\sigma=(S_1,S_2,\ldots,S_N)$ can then be conveniently calculated using the following Ising-type Hamiltonian:

$$\Delta H_{\mathrm{CE}}(\sigma)=\sum_f D_f J_f \bar{\Pi}_f(\sigma), \tag{2}$$

where f is a figure (cluster) comprised of a group of lattice sites (single site, pairs, triplets, etc.), D_f is the degeneracy factor indicating the number of figures of type f per f.u., J_f is the configuration-independent Ising-type interaction energy for figure f called effective cluster interaction (ECI), and $\bar{\Pi}_f$ is the correlation function defined as the product of the spin variables over all sites of a figure, averaging over all symmetry-equivalent figures of the lattice. Once $\{J_f\}$ is known one can readily use Eq. (2) to predict the formation energy of any configuration, both ordered and disordered, with the accuracy of first-principles calculations. Note that the effects of local atomic relaxations can be readily incorporated into Eq. (2) as long as there is a one-to-one correspondence between lattice sites and atomic positions.

The expansion in Eq. (2) is exact as long as *all* the figures are included. However, in practice, since the interactions between widely separated atoms are expected to be weaker than interactions between nearer ones, the expansion in Eq. (2) can usually be truncated at certain distance to include only a few short-ranged pair and multisite clusters. In the present study, we determine $\{J_f\}$ by fitting $\Delta H_{\mathrm{CE}}(\sigma_{\mathrm{ord}})$ to first-principles calculated formation energies $\Delta H_{\mathrm{FP}}(\sigma_{\mathrm{ord}})$ of a set $\{\sigma_{\mathrm{ord}}\}$ of 46 input Co_3AlC_x ordered structures (not necessarily ground states) containing up to 49 atoms per unit cell. The Co and Al atoms do not have occupational degree of freedom and are not explicitly included in the cluster expansion. Their effects are however implicitly included in $\Delta H_{\mathrm{FP}}(\sigma_{\mathrm{ord}})$ and thus $\{J_f\}$. A well-converged cluster expansion is obtained using five pair, five triple, and five quadruplet interactions with an average fitting error of 5.8 meV/f.u. (or ~1.3 meV/atom). To further assess the predictive power of our cluster expansion, we also calculate its cross-validation (cv) score, defined as

$$\mathrm{cv}^2=\frac{1}{N}\sum_{i=1}^{N}(\Delta H_i^{\mathrm{FP}}-\Delta H_i^{\mathrm{CE}})^2, \tag{3}$$

where ΔH_i^{FP} is the first-principles calculated formation energy of structure i, while ΔH_i^{CE} is the formation energy of structure i predicted from a cluster expansion constructed using the calculated formation energies of the other $N-1$ structures. The cv score of our cluster expansion is found to be only 9.6 meV/f.u. (or ~2.1 meV/atom).

The final obtained ECIs of our cluster expansion are given in Table I, together with the definitions of all the figures considered. The dominating interaction is a repulsive nearest-neighbor pair interaction $(J_2>0)$ since its symmetry-

weighted value ($D_f J_f$) is clearly the largest among all interactions. This strongly indicates a tendency toward vacancy ordering rather than vacancy clustering in Co_3AlC_x alloys. Indeed, the formation energies of all the ordered structures considered here are negative. It is worth noting that although vacancies tend to avoid each other as nearest neighbors, they actually prefer the second-nearest-neighbor separation distance due to an attractive second-nearest-neighbor pair interaction ($K_2 < 0$), which is precisely what has been observed experimentally.[3–5]

III. RESULTS AND DISCUSSIONS

A. Site preference of C in $L1_2Co_3Al$

The perovskite $E2_1$ structure can also be viewed as carbon atoms occupying the octahedral interstices of the $L1_2$ lattice formed by Co and Al atoms. Here C atoms exclusively occupy the octahedral interstices at cube center, leaving all the octahedral interstices at cube edges vacant. It may be argued that entropy-driven occupation of those edge octahedral sites may occur at high temperatures, which cannot be described by the present cluster expansion. To explore such a possibility, we have performed first-principles calculations on two 32-atom $2\times2\times2$ $L1_2Co_3Al$ supercells: one contains a C atom at a center octahedral site and one contains a C atom at an edge octahedral site. The site preference energy, defined as the total-energy difference between those two fully relaxed supercells, turns out to be 1.84 eV, which indicates that C has a very strong preference for the center octahedral site in Co_3Al. Such a large energy difference is unlikely to be overcome by the comparatively smaller entropic effects at finite temperatures. Thus, those edge octahedral sites can be safely neglected in our study.

The origin of the strong site preference may be understood in terms of both electronic and size effects. Since a center octahedral site is surrounded by six nearest-neighbor Co atoms, while an edge octahedral site is surrounded by two Al atoms and four Co atoms, putting C atoms in center octahedral sites may promote better bonding between Co and C atoms. Indeed, previous electronic density-of-states calculations by Ohtani *et al.*[18] indicate that there is a hybridization between Co *d* states and Co *p* states in the $E2_1$-Co_3AlC structure, an evidence of covalent Co-C bonds. Furthermore, since Al atom is larger than Co atom, a center octahedral site will have a larger "radii" than an edge octahedral site and thus putting C atoms in center octahedral sites also minimizes the strain energy.

B. Finding the ground states

To answer the question what are the most stable vacancy-ordered structures, we have performed an exhaustive direct enumeration ground-state search[19] among all the possible $E2_1$-based structures up to 70 atoms (14 1*b* sites) per unit cell with our cluster expansion Hamiltonian, and our results are shown in Fig. 2. In order for a structure to be ground state, it not only needs to be the lowest-energy structure at a given composition but also needs to be stable with respect to phase separation into competing structures at other compositions. Out of a total of $\sim4\times10^4$ possible candidate structures, our search revealed two ground-state structures in the proximity of the experimentally observed composition of $Co_3AlC_{0.59}$: a cubic $Co_3AlC_{0.5}$ (space group $Fm\bar{3}m$, No. 225) phase and a trigonal $Co_3AlC_{0.667}$ (space group $P\bar{3}m1$, No. 164) phase. Their lattice parameters and internal atomic coordinates are further given in Tables II and III, respectively. Both structures are also the ground states among the 46 input structures according to direct first-principles calculations. As shown in Fig. 3, the unit cell of $Co_3AlC_{0.5}$ is based on $2\times2\times2$ $E2_1$ Co_3AlC supercell with half of the carbon atoms missing, while the unit cell of $Co_3AlC_{0.667}$ is based on $3\times3\times3$ $E2_1$ Co_3AlC supercell with one-third of the carbon atoms missing. In both structures, the vacancies are arranged in a way such that no two vacancies become nearest neighbors. Instead, they are all separated by second-nearest-neighbor distance, which is energetically favorable as discussed previously. Remarkably, the predicted $Co_3AlC_{0.5}$ ground state has actually been experimentally observed by

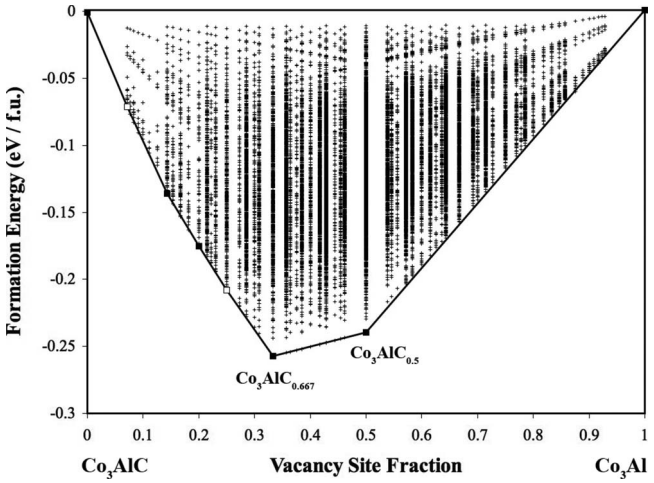

FIG. 2. Exhaustive ground-state search ($\sim4\times10^4$ structures) using the cluster expansion technique. The lowest-energy stable vacancy-ordered compounds are shown as squares. Some of the predicted ground states are already included in our original set of GGA-calculated energies (filled squares), but some are not (empty squares) and are therefore truly unsuspected predictions by the cluster expansion.

TABLE II. First-principles predicted equilibrium lattice parameters of $Co_3AlC_{0.5}$ and $Co_3AlC_{0.667}$ phases.

Phase	Structure	*a* (Å)	*b* (Å)	*c* (Å)	α	β	γ
$Co_3AlC_{0.5}$	Cubic	7.262	7.262	7.262	90°	90°	90°
$Co_3AlC_{0.667}$	Trigonal	5.167	5.167	6.338	90°	90°	120°

TABLE III. First-principles calculated cell internal parameters of $Co_3AlC_{0.5}$ and $Co_3AlC_{0.667}$ phases.

Phase	Wyckoff position	x	y	z
$Co_3AlC_{0.5}$	Al:8c	0.25	0.25	0.25
	Co:24e	0.5	0.5	0.2418
	C:4b	0.5	0.5	0.5
$Co_3AlC_{0.667}$	Al1:1a	0	0	0
	Al2:2d	1/3	2/3	0.3364
	Co1:3e	0.5	0	0
	Co2:6i	0.1604	0.3208	0.6591
	C2:6	1/3	2/3	0.8167

Mishima and co-workers[3–5] using electron diffraction, which further underlines the accuracy of the present cluster expansion.

To verify that those two structures are true ground states, we also subject our cluster expansion to Monte Carlo simulate-annealing simulations.[19] Monte Carlo simulations are performed within a canonical ensemble, i.e., fixed composition. For $x=1/2$, a large $16\times16\times16$ cubic simulation cell is used that contains 4096 Al atoms, 12288 Co atoms, and a total of 4096 C atoms and vacancies (with periodic boundary conditions). For $x=2/3$, a large $18\times18\times18$ cubic simulation cell is used that contains a total of 5832 C atoms and vacancies. For each simulation, we start from a high temperature for a substitutionally random state (an extremely high temperature of 50 000 K is used to obtain the truly random state of the alloy since at such high temperature, almost all the atom exchanges in the Metropolis algorithm will be accepted) and slowly cool the system down to a low temperature at which all configurational changes prove to be energetically unfavorable. This gives: (1) the $T=0$ K ground-state structures and (2) the order-disorder transition temperatures. Our simulated annealing simulations show that $Co_3AlC_{0.5}$ and $Co_3AlC_{0.667}$ are not only the ground states out of all structures with up to 70 atoms per unit cell but are also truly the lowest-energy configurations out of an astronomical number of possible configurations [without symmetry, there are $N_{conf}=N!/(xN)!(N-xN)!$ of possible configurations that can be explored in our Monte Carlo simulations, where N is the total number of 1b sites in simulation cell].

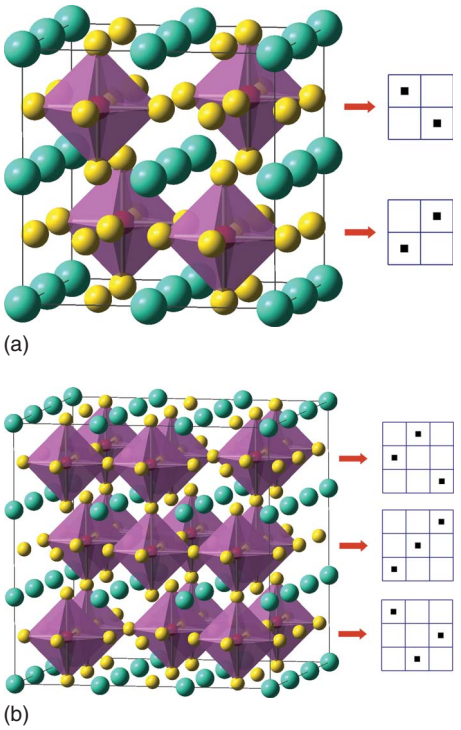

FIG. 3. (Color online) Unit cells of (a) cubic $Co_3AlC_{0.5}$ and (b) trigonal $Co_3AlC_{0.667}$ structures. Cyan, yellow, and red spheres represent Al, Co, and C atoms, respectively. The ordered patterns of carbon vacancies (black squares) are also shown.

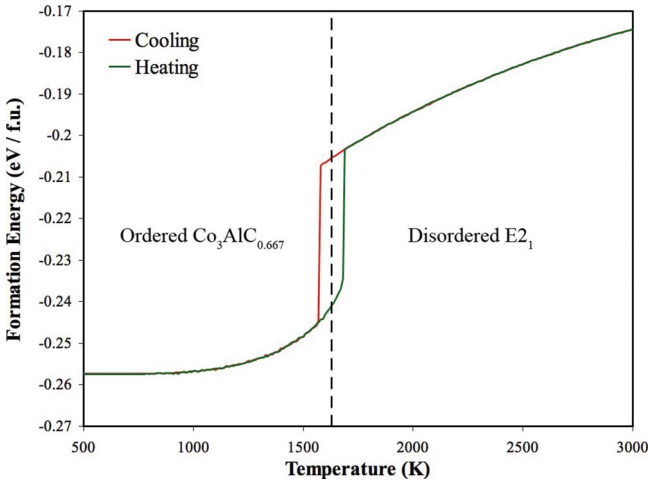

FIG. 4. (Color online) Formation energy of $Co_3AlC_{0.667}$ alloy as a function of temperature from Monte Carlo simulated annealing. Results obtained from Monte Carlo heating simulations are also shown.

C. Order-disorder transition temperatures

As shown in Fig. 4, the order-disorder transition between the low-temperature ordered $Co_3AlC_{0.667}$ phase and the high–temperature-disordered $E2_1$ phase occurs at ~1630 K. Such a transition is clearly of first order in view of the discontinuity in energy vs temperature curve. The discrepancies between cooling and heating curves are due to hysteresis typical of first-order phase transitions. For $Co_3AlC_{0.5}$, the cooling and heating energy curves overlap with each other [see Fig. 5(a)], suggesting that the transition is of second order. By monitoring peaks in heat capacity vs temperature curve [see Fig. 5(b)], its order-disorder temperature is predicted to be ~1925 K. The lower transition temperature of $Co_3AlC_{0.667}$ may explain why it has not yet been observed experimentally. Therefore, we assert that further experimental examination of the lower-temperature phase stability of Co_3AlC_x alloys would be of interest.

Our predicted order-disorder temperature of $Co_3AlC_{0.5}$ is ~600 K higher than experiments [~1325 K (Ref. 4)]. Such a discrepancy may be attributed to the fact that the ECIs used in our Monte Carlo simulations are obtained from first-principles calculations at $T=0$ K and are assumed to be tem-

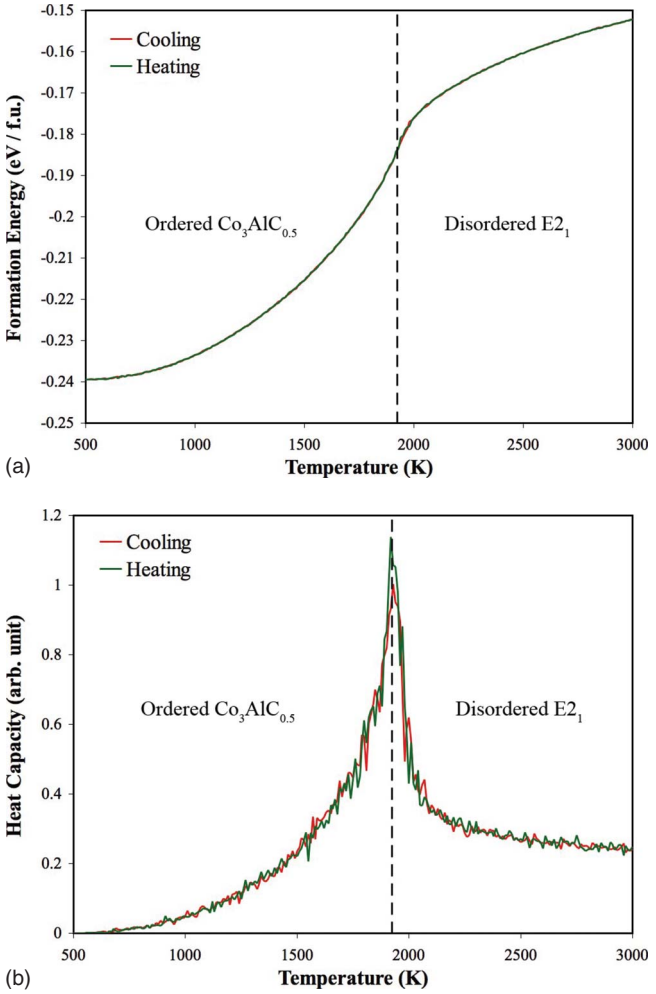

FIG. 5. (Color online) Formation energy (a) and heat capacity (b) of $Co_3AlC_{0.5}$ alloy as a function of temperature from Monte Carlo simulated annealing. Results obtained from Monte Carlo heating simulations are also shown.

perature independent. As the consequence, the effects of nonconfigurational contributions (lattice vibrations, electronic excitations, etc.) to the free energy are neglected in the present study, which may shift the order-disorder temperatures. Other possible reasons for such a discrepancy may be due to the inaccuracies of first-principles calculations as well as the fitting errors of our cluster expansion.

D. Mixing energies of disordered Co_3AlC_x alloys

For a perfectly random $(T\rightarrow\infty)A_{1-x}B_x$ alloy, there is no correlation in the occupation between various sites, and therefore the pair and multisite correlation function $\bar{\Pi}_f$ can be simply written as the product of the lattice-averaged site variable $\langle S_i\rangle=2x-1$, i.e., $\langle\bar{\Pi}_f\rangle_R=(2x-1)^2$ for pair and $\langle\bar{\Pi}_f\rangle_R=(2x-1)^3$ for triple interactions. Therefore, the mixing energy of a random $A_{1-x}B_x$ alloy can be calculated analytically from the cluster expansion as

$$\Delta H(x)=\langle\Delta H_{\mathrm{CE}}(\sigma)\rangle_R=\sum_f D_f J_f(2x-1)^{k_f}, \qquad (4)$$

where k_f is the number of vertices in figure f. Using Eq. (4), the mixing energies (per f.u.) of random $E2_1$ Co_3AlC_x alloys

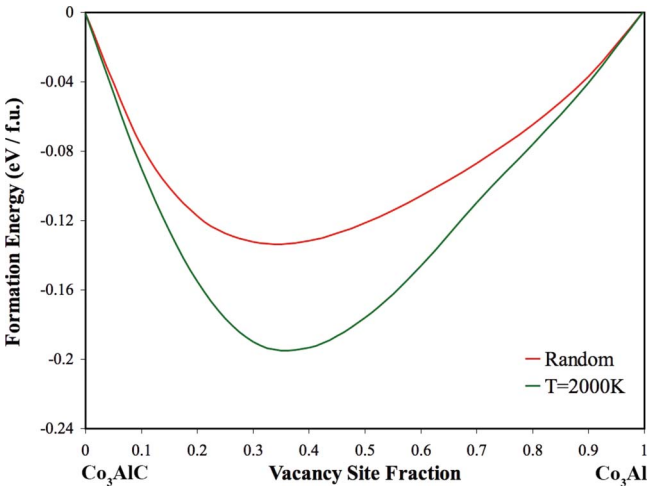

FIG. 6. (Color online) Mixing energy of perfectly random $(T\rightarrow\infty)Co_3AlC_x$ alloy as a function of composition predicted from the present cluster expansion. Monte Carlo simulated mixing energies of disordered Co_3AlC_x alloys at $T=2000$ K are also shown.

are calculated as a function of composition (see Fig. 6). Such data are quite useful for the development of thermodynamic database for Co-Al-C ternary system using the calculation of phase diagrams (CALPHAD) approach.[18] For comparison, we have also obtained the mixing energies of disordered Co_3AlC_x alloys at $T=2000$ K by performing Monte Carlo simulations in a large $20\times20\times20$ cubic simulation cell. As can be seen, short-range ordering (SRO) effects play an important role in stabilizing the Co_3AlC_x solid solution at finite temperatures. At all alloy compositions and temperatures, the mixing energy of disordered Co_3AlC_x alloy remains negative, which is consistent with the ordering tendency in this alloy.

E. Phase stability of Co_3AlC_x alloys

It is useful to apply the present cluster expansion to gain valuable insight into the phase stability of Co_3AlC_x alloys in the Co-Al-C ternary system. As an example, here we consider the stability of disordered $E2_1$ Co_3AlC_x alloys at $T=2000$ K. We calculate their heats of formation (per atom) using the constituent pure elements as reference states,

$$E_{\mathrm{form}}=\frac{E(\mathrm{Co_3AlC}_x)-3E(\mathrm{Co})-E(\mathrm{Al})-xE(\mathrm{C})}{4+x}, \qquad (5)$$

where E(Co), E(Al), and E(C) are, respectively, the first-principles calculated total energies (per atom) of ferromagnetic hcp Co, fcc Al, and graphite. $E(Co_3AlC_x)$ is the total energy (per f.u.) of a disordered Co_3AlC_x alloy as obtained from finite-temperature Monte Carlo simulations.

Figure 7 shows the heats of formation of disordered Co_3AlC_x alloys at $T=2000$ K as a function of composition. Without carbon ($x=0$), the $L1_2$ Co_3Al structure is thermodynamically unstable with respect to phase separation into a mechanical mixture of $B2$ CoAl and hcp Co. Such a conclusion agrees with a recent first-principles study by Mihalkovic and Widom,[20] and also the fact that no stable $L1_2$ Co_3Al

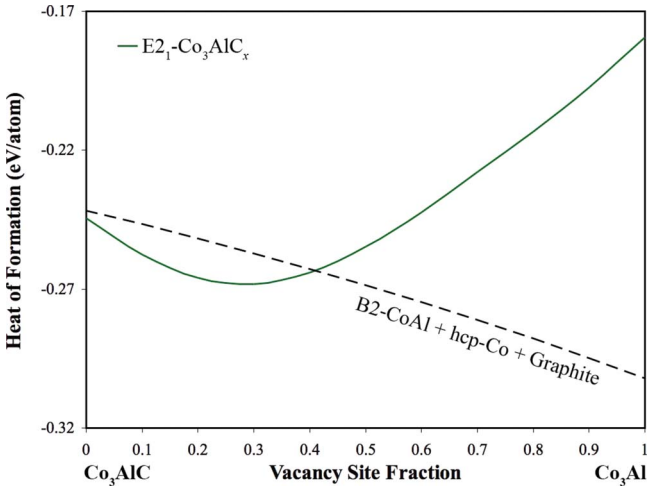

FIG. 7. (Color online) Heat of formation of disordered Co_3AlC_x alloy at $T=2000$ K as a function of composition. For the purpose of comparison, the heat of formation of a mechanical mixture of $B2$ CoAl, hcp Co, and graphite with the same alloy composition is shown as a dashed line.

compound has been observed in the Co-Al system.[1] However, with increasing C concentration, the heat of formation of Co_3AlC_x alloy rapidly decreases. When $x>0.6$, the disordered Co_3AlC_x alloy already has lower energy than that of a mechanical mixture of the three ground-state structures in the Co-Al-C ternary system:[5,18] $B2$ CoAl, hcp Co, and graphite. We thus conclude that the formation of the $E2_1$ Co_3AlC_x alloy is stabilized by the addition of carbon. It is also interesting to note that the minimum in the heat of formation vs composition curve does not occur at $x=1$, which may explain why the experimentally observed Co_3AlC_x is nonstoichiometric.

IV. SUMMARY

To investigate vacancy ordering in Co_3AlC_x alloys, we parametrize first-principles calculated total energies of 46 ordered structures into a cluster expansion that is capable of predicting energetics of any $1b$-site vacancy configuration. Near the experimentally observed composition of $Co_3AlC_{0.59}$, our exhaustive ground-state search identifies $Co_3AlC_{0.5}$ and $Co_3AlC_{0.667}$ as the two stable vacancy-ordered structures, and the former has been experimentally observed. The order-disorder transition temperatures of those two structures are found by Monte Carlo simulations to be $\sim$1925 and $\sim$1630 K, respectively. The lower order-disorder temperature of $Co_3AlC_{0.667}$ may explain why this phase has not yet been observed experimentally. Using our cluster expansion, the mixing energies of random and disordered $E2_1$ $Co3AlC_x$ alloys are also predicted in our study.

ACKNOWLEDGMENTS

The author wishes to thank Axel van de Walle for providing ATAT software package. This work is financially supported by Director's postdoctoral program at Los Alamos National Laboratory (LANL). All calculations were performed using the parallel computing facilities at LANL.

*Corresponding author; chao@lanl.gov

[1] T. B. Massalski, *Binary Alloy Phase Diagrams*, 2nd ed. (ASM, Metal Park, OH, 1990).
[2] L. J. Huetter and H. H. Stadelmaier, Acta Mater. **6**, 367 (1958).
[3] Y. Mishima, K. Y. Hwang, and F. G. Wei, *High-Temperature Ordered Intermetallic Alloys VIII*, MRS Symposia Proceedings No. 552 (Materials Research Society, Pittsburgh, 1999), p. KK7.8.1.
[4] Y. Kimura, K. Sakai, F. G. Wei, and Y. Mishima, Intermetallics **14**, 1262 (2006).
[5] Y. Kimura, K. Iida, F. G. Wei, and Y. Mishima, Intermetallics **14**, 508 (2006).
[6] A. A. Rempel, Phys. Usp. **39**, 31 (1996).
[7] P. A. Korzhavyi, L. V. Pourovskii, H. W. Hugosson, A. V. Ruban, and B. Johansson, Phys. Rev. Lett. **88**, 015505 (2001).
[8] R. Eibler, J. Phys.: Condens. Matter **19**, 196226 (2007).
[9] J. M. Sanchez, F. Ducastella, and D. Gratias, Physica A **128**, 334 (1984).
[10] J. W. D. Connolly and A. R. Williams, Phys. Rev. B **27**, 5169 (1983).
[11] D. B. Laks, L. G. Ferreira, S. Froyen, and A. Zunger, Phys. Rev. B **46**, 12587 (1992).
[12] C. Wolverton and A. Zunger, Phys. Rev. Lett. **75**, 3162 (1995).
[13] A. Zunger, L. G. Wang, G. L. W. Hart, and M. Sanati, Modell. Simul. Mater. Sci. Eng. **10**, 685 (2002).
[14] G. Kresse and D. Joubert, Phys. Rev. B **59**, 1758 (1999).
[15] G. Kresse and J. Furthmuller, Comput. Mater. Sci. **6**, 15 (1996).
[16] J. P. Perdew, K. Burke, and M. Ernzerhof, Phys. Rev. Lett. **77**, 3865 (1996).
[17] H. J. Monkhorst and J. D. Pack, Phys. Rev. B **13**, 5188 (1972).
[18] H. Ohtani, M. Yamano, and M. Hasebe, CALPHAD: Comput. Coupling Phase Diagrams Thermochem. **28**, 177 (2004).
[19] Z. W. Lu, D. B. Laks, S. H. Wei, and A. Zunger, Phys. Rev. B **50**, 6642 (1994).
[20] M. Mihalkovic and M. Widom, Phys. Rev. B **75**, 014207 (2007).